

Role of DC-SIGN in Lassa Virus Entry into Human Dendritic Cells

Ana-Rita Goncalves,^a Marie-Laurence Moraz,^a Antonella Pasquato,^a Ari Helenius,^b Pierre-Yves Lozach,^c Stefan Kunz^a

Institute of Microbiology, Lausanne University Hospital and University of Lausanne, Lausanne, Switzerland^a; Institute of Biochemistry, Federal Institute of Technology, Zurich (ETHZ), Zurich, Switzerland^b; INRS-Institut Armand-Frappier, Université du Québec, Laval, Québec, Canada^c

The arenavirus Lassa virus (LASV) causes a severe hemorrhagic fever with high mortality in humans. Antigen-presenting cells, in particular dendritic cells (DCs), are early and preferred targets of LASV, and their productive infection contributes to the virus-induced immunosuppression observed in fatal disease. Here, we characterized the role of the C-type lectin DC-specific ICAM-3-grabbing nonintegrin (DC-SIGN) in LASV entry into primary human DCs using a chimera of the prototypic arenavirus lymphocytic choriomeningitis virus (LCMV) expressing the LASV glycoprotein (rLCMV-LASVGP). We found that differentiation of human primary monocytes into DCs enhanced virus attachment and entry, concomitant with the upregulation of DC-SIGN. LASV and rLCMV-LASVGP bound to DC-SIGN via mannose sugars located on the N-terminal GP1 subunit of LASVGP. We provide evidence that DC-SIGN serves as an attachment factor for rLCMV-LASVGP in monocyte-derived immature dendritic cells (MDDC) and can accelerate the capture of free virus. However, in contrast to the phlebovirus Uukuniemi virus (UUKV), which uses DC-SIGN as an authentic entry receptor, productive infection with rLCMV-LASVGP was less dependent on DC-SIGN. In contrast to the DC-SIGN-mediated cell entry of UUKV, entry of rLCMV-LASVGP in MDDC was remarkably slow and depended on actin, indicating the use of different endocytotic pathways. In sum, our data reveal that DC-SIGN can facilitate cell entry of LASV in human MDDC but that its role seems distinct from the function as an authentic entry receptor reported for phleboviruses.

The arenavirus Lassa virus (LASV) is endemic in western Africa from Senegal to Cameroon and causes several hundred thousand infections per year with high mortality (1). There is currently no vaccine available, and therapeutic intervention is limited to intensive care and the use of ribavirin, which shows some efficacy when given early in the disease (2). Considering the number of people affected, the human suffering involved, and the unaddressed need for better therapeutics, LASV is arguably one of the most neglected tropical pathogens.

A highly predictive factor for the outcome of LASV infection in humans is the extent of viremia (3). Patients with fatal Lassa fever have higher viral loads at the time of hospitalization and are unable to limit viral spread, whereas survivors have lower viral loads and control infection progressively. The inability of the host to control viral infection in fatal Lassa fever cases is due to a marked virus-induced immunosuppression (1). The virus-induced immunosuppression likely involves infection of antigen-presenting cells (APCs), in particular dendritic cells (DCs), which are crucial for the development of the adaptive antiviral immune response in a primary LASV infection (4). Accordingly, infection of human DCs with LASV fails to activate the cells and results in impairment of their ability to present antigens to T cells (5, 6). However, the virus-induced mechanisms leading to immunosuppression remain largely unknown.

Arenaviruses are enveloped negative-strand RNA viruses with a cell cycle restricted to the cytoplasm (7–9). The viral genome is comprised of two RNA segments. The S segment encodes the envelope glycoprotein (GP) precursor (GPC) and the nucleoprotein (NP), and the L segment encodes the matrix protein (Z), as well as the viral polymerase (L). The viral GPC is synthesized as a single polypeptide and undergoes processing by cellular proteases, yielding the N-terminal GP1, the transmembrane GP2, and a stable signal peptide (SSP) (10). GP1 binds to cellular receptors (11), whereas GP2 mediates viral fusion and structurally resembles

other class I viral fusion proteins (12, 13). The first cellular receptor discovered for LASV was dystroglycan (DG), a ubiquitously expressed receptor for extracellular matrix (ECM) proteins (14, 15). Recent efforts to discover novel cellular receptors for LASV using an expression-cloning approach identified the Tyro3/Axl/Mer (TAM) receptor tyrosine kinases Axl and Dtk (Tyro3), as well as the C-type lectins DC-specific ICAM-3-grabbing nonintegrin (DC-SIGN) and LSECtin, as novel candidate receptors (16).

DC-SIGN is a type II C-type lectin that contains a carbohydrate recognition domain that binds pathogen-derived high-mannose carbohydrates in a calcium-dependent manner. DC-SIGN is present on many classes of DCs, and its expression can be subject to regulation by different factors (17, 18). In DCs, DC-SIGN is normally involved in endocytosis of antigens and delivery to late endosomes/lysosomes, followed by processing and subsequent presentation in the context of major histocompatibility complex class II (MHC-II) (19). DC-SIGN can facilitate infection or transmission of a variety of enveloped viruses, such as HIV-1 (20, 21), the filoviruses Ebola virus and Marburg virus (22, 23), severe acute respiratory syndrome (SARS) coronavirus (24), and the flaviviruses dengue virus (25, 26) and West Nile virus (27). Recently, DC-SIGN has been identified as the cell entry receptor for arthropod-borne bunyaviruses of the genus *Phlebovirus*, including Rift Valley fever virus (RVFV) and Uukuniemi virus (UUKV), in human DCs (28). DC-SIGN was found to directly bind to high-mannose glycans on phlebovirus GPs and to be crucial for attach-

Received 10 July 2013 Accepted 10 August 2013

Published ahead of print 21 August 2013

Address correspondence to Stefan Kunz, Stefan.Kunz@chuv.ch.

Copyright © 2013, American Society for Microbiology. All Rights Reserved.

doi:10.1128/JVI.01893-13

ment and subsequent internalization, leading to productive infection. Considering the crucial role of human DCs in the development of an antiviral immune response, the mechanisms by which LASV invades these cells are of particular interest in understanding the viral pathogenesis. In our present study, we investigated the roles of known candidate receptors for LASV entry into human DCs.

MATERIALS AND METHODS

Antibodies and reagents. Monoclonal antibodies (MAbs) 113 (anti-*LCMVNP*) and 83.6 (anti-*LCMVGP*) have been described previously (29, 30). Mouse MAb B-ly6 anti-CD11c conjugated to phycoerythrin (PE), mouse MAb 2331 anti-CD86-PE, mouse MAb DCN46 anti-CD209 (DC-SIGN)-PE, and mouse MAb M5E2 anti-CD14-PE were from BD Pharmingen. Purified polyclonal goat IgG anti-human Axl (hAxl), MAb 125518 anti-hMer-PE, MAb 96201 anti-hDtk-PE, MAb 120507 anti-DC-SIGN, and MAb DC28 anti-DC-SIGN/DC-SIGNR were from R&D Systems. Polyclonal guinea pig anti-*LCMVNP* serum was provided by Juan Carlos de la Torre (Scripps Research Institute, La Jolla, CA). The rabbit polyclonal antibody U2 is directed against all UUKV proteins and was generated as previously described (31). Mouse MAb B-5-1-2 anti- α -tubulin, rabbit anti-goat IgG, goat anti-mouse IgG secondary antibodies conjugated to PE, and biotinylated anti-guinea pig IgG were purchased from Sigma-Aldrich. Horseradish peroxidase (HRP)-conjugated polyclonal rabbit anti-mouse IgG was from Dako and Rhodamine Red-X-AffiniPure F(ab')₂ Fragment Goat Anti-Rabbit IgG (H+L) was from Jackson ImmunoResearch (European Union), while Alexa Fluor 594 goat anti-mouse IgM (μ chain), Alexa Fluor 594 streptavidin, and 4',6-diamidino-2-phenylindole (DAPI) were purchased from Molecular Probes (Invitrogen). Human FcR blocking reagent (MACS, Miltenyi Biotec) was used during surface staining of immature dendritic cells with "whole" IgG primary antibodies.

Recombinant human granulocyte-macrophage colony-stimulating factor (GM-CSF) and recombinant human interleukin-4 (IL-4) were obtained from Gibco. A recombinant human DC-SIGN/CD209/Fc chimera was from R&D Systems, and β 1-2-*N*-acetylglucosamine-mannose (GlcNAc β 1-2man) was from Dextra Inc. The LIVE/DEAD fixable dead cell stain kit was from Molecular Probes, Invitrogen. Recombinant DG fused to human IgG Fc (DG-Fc) was produced as described previously (32).

Cells and viruses. Peripheral blood mononuclear cells (PBMCs) were isolated from human blood obtained from healthy volunteers (the protocol was approved by the Commission Cantonale d'Éthique de la Recherche sur l'Être Humain of the Canton de Vaud, number 106/10) or from buffy coats (provided by the Service Régional Vaudois de Transfusion Sanguine, Epalinges, Switzerland) or purchased as frozen aliquots from Clonethics/Lonza (Walkersville, MD). Briefly, blood samples or buffy coats were diluted to 2 to 4 times the volume in phosphate-buffered saline (PBS) supplemented with 2 mM EDTA Ultrapure (Gibco) and transferred in Leucosep tubes (Greiner Bio-One GmbH) previously loaded with Bio-coll Separating Solution at 1.077-g/ml density (Biochrom AG) according to the manufacturer's instructions. The Leucosep tubes were then centrifuged at 1,000 \times g for 10 min at 20°C in a swinging-bucket rotor without a brake. The plasma layer was discarded, and the PBMC "ring" was collected, washed once with PBS-EDTA, and centrifuged for 10 min at 300 \times g. The red blood cells were lysed using sterile ACK lysis buffer (1 mM KHCO₃, 0.15 M NH₄Cl, 0.1 mM EDTA, HCl, pH 7.2 to 7.4) for 3 to 4 min. The cells were washed again with PBS-EDTA and centrifuged at 200 \times g for 15 min at 4°C. CD14⁺ monocytes were isolated from PBMCs by CD14⁺ positive selection using a magnetic cell sorter (MACS, Miltenyi Biotec) according to the manufacturer's instructions. Monocyte-derived immature dendritic cells (MDDC) were obtained by culturing CD14⁺ monocytes in RPMI 1640 medium plus GlutaMax (Gibco) supplemented with 10% fetal calf serum (FCS), antibiotics (100 U/ml penicillin and 0.1 mg/ml streptomycin), 100 ng/ml GM-CSF, and 50 ng/ml IL-4 for 3 to 5

days, as described previously (33). A549 and HEK293 cells were cultured in Dulbecco's modified Eagle's medium (DMEM)-10% (vol/vol) fetal bovine serum (FBS) supplemented with glutamine and penicillin-streptomycin. Jurkat cells were maintained in RPMI-10% (vol/vol) FBS supplemented with glutamine and penicillin-streptomycin. Raji cell lines expressing DC-SIGN wild type (WT) and a DC-SIGN-LL mutant were maintained in RPMI 1640 medium plus GlutaMax supplemented with 10% FCS, 100 U/ml penicillin, and 0.1 mg/ml streptomycin as described previously (34). The Raji-derived B-THP-1 cells expressing LSECTin were a gift from the laboratory of Stefan Pöhlmann, Deutsches Primatenzentrum, Göttingen, Germany, and were maintained as described previously (35).

The recombinants rLCMV-LASVGP and rLCMV-VSVG have been described elsewhere (36, 37). According to the institutional biosafety guidelines of the Lausanne University Hospital, the chimera rLCMV-LASVGP has been classified as a biosafety level 2 (BSL2) pathogen for use in cell culture. The generation of recombinant VSV Δ G* expressing green fluorescent protein (GFP) pseudotyped with VSV G protein (rVSV Δ G*-VSVG) has been reported previously (38, 39). Viruses were produced, and the titers were determined as previously described (40). UUKV strain S23 was used in this study (41). UUKV production, purification, and titration were performed in mammalian BHK-21 cells as described previously (28, 31). LASV (strain Josiah) was produced at the Special Pathogens Branch of the Centers for Disease Control and Prevention (Atlanta, GA) and inactivated by gamma irradiation using a dose of 2 \times 10⁶ rads, as described previously (42).

Flow cytometry analysis. For cell surface staining, cells were detached, when adherent, with enzyme-free cell dissociation solution, resuspended in fluorescence-activated cell sorting (FACS) buffer (1% [vol/vol] FCS, 0.1% [wt/vol] sodium azide, PBS), and plated in conical 96-well plates, followed by 1 h on ice with FACS buffer diluted with the corresponding primary antibody. The cells were then washed twice in FACS buffer and labeled with secondary antibodies (as needed) for 45 min on ice in the dark. After two wash steps in 1% (vol/vol) FBS in PBS, the cells were fixed with 1/10 CellFix solution for 10 min at room temperature (RT) in the dark. The cells were washed twice with PBS, and the fluorescence intensity was assessed using a FACSCalibur flow cytometer (Becton, Dickinson) with CellQuest Pro acquisition and analysis software. Intracellular FACS staining of *LCMVNP* and UUKV antigens was performed as described previously (43).

Solid-phase binding assays. For binding of virus to DC-SIGN-Fc and DG-Fc fusion proteins, 20 μ g/ml purified proteins in PBS was immobilized in microtiter plates for 2 h, and nonspecific binding was blocked with 1% (wt/vol) bovine serum albumin (BSA) in PBS. Inactivated LASV or rLCMV-LASVGP (10⁷ PFU/ml) in 1% (wt/vol) BSA-PBS was applied for 12 h at 6°C. Bound viruses were detected with MAb 83.6 (20 μ g/ml) in 1% (wt/vol) BSA-PBS using an HRP-conjugated secondary antibody. For binding of DC-SIGN and DG-Fc fusion proteins to rLCMV-LASVGP, purified viruses (10⁷ PFU/ml) were immobilized in microtiter plates and incubated with the Fc fusion proteins for 2 h at 4°C. Bound Fc fusion proteins were detected with a combination of mouse anti-human IgG Fc (1:500) and HRP-conjugated goat anti-mouse IgG (1:500). Assays were developed with ABTS [2,2 α -azinobis(3-ethylbenzthiazolinesulfonic acid)] substrate, and the optical density at 405 nm (OD₄₀₅) was recorded in an enzyme-linked immunosorbent assay (ELISA) reader. Background binding to BSA was subtracted.

Virus binding to monocytes and MDDC. For biotinylation of rLCMV-LASVGP, we used a modified version of the protocol described previously (44). Briefly, purified virus was dialyzed against reaction buffer (0.1 M NaHCO₃, 100 mM NaCl, pH 8.0) and reacted twice with 1 mM NHS-X-biotin (Calbiochem) for 20 min on ice. The reaction was quenched by adding cold 50 mM (final concentration) glycine, pH 8.0, for 10 min; the virus was dialyzed against PBS; and infectivity was checked by immunofocus assay (IFA) on VeroE6 cells. Only biotinylated virus retaining >50% infectivity was used in experiments. For virus binding assays,

single-cell suspensions of monocytes and MDDC were prepared in 1% (vol/vol) FBS, 0.1% (wt/vol) sodium azide, PBS supplemented with 1 mM MgCl₂ and 0.5 mM CaCl₂ (binding buffer) and blocked for 15 min on ice. Cells (5×10^4 per well) were transferred to M96 plates (Costar), centrifuged for 5 min at 1,200 rpm, and resuspended in 50 μ l binding buffer containing biotinylated rLCMV-LASVGP at the indicated particle/cell ratios in the presence or absence of inhibitors. Incubation was performed for 1 h on ice under shaking. After two wash steps in binding buffer, the cells were resuspended in 4% (wt/vol) paraformaldehyde in PBS with 1 mM MgCl₂ and 0.5 mM CaCl₂ and fixed for 20 min on ice. After three washes in binding buffer, biotinylated virus was detected by adding fluorescein isothiocyanate (FITC)-conjugated streptavidin (1:100 in binding buffer) for 45 min in the dark. After three wash steps, the cells were fixed with 4% (wt/vol) paraformaldehyde-PBS for 10 min at room temperature, washed twice with PBS, and analyzed with a FACSCalibur flow cytometer (Becton, Dickinson, San Jose, CA) using CellQuest software.

Infection and inhibitor studies in Raji and B-THP-1 cells. Raji cells were seeded in round-bottom 96-well plates (Costar) and pretreated for 30 min in the presence of mannan, anti-DC-SIGN antibodies (120507 or DC28), and 5 mM EDTA/EGTA at the indicated concentrations at 37°C, followed by 1 h of infection at 37°C with rLCMV-LASVGP or UUKV at the indicated multiplicity of infection (MOI) in the presence of the inhibitors at 37°C. Unbound virus was removed by washing the cells. At 4 h postinfection, 20 mM ammonium chloride was added to prevent secondary infection. At 16 h postinfection, the cells were fixed (BD cellFix). Infection with rLCMV-LASVGP was assessed by intracellular staining of LCMVNP with MAb 113 and a PE-conjugated secondary antibody, followed by analysis in flow cytometry as described previously (43). Infection with UUKV was assessed by flow cytometry at 7 h postinfection as described previously (28). B-THP-1 cells were seeded at 10^4 cells/well in round-bottom 96-well plates and incubated with the indicated concentrations of inhibitors for 30 min. Cells were infected with rLCMV-LASVGP and rLCMV-VSVG at an MOI of 10 as described above, and infection was assessed after 16 h by flow cytometry.

Determination of viral attachment and entry kinetics in MDDC. To assess the kinetics of viral attachment, MDDC were seeded in round-bottom 96-well plates. After 16 h, the cells were chilled in ice and pretreated with MAb DC28 or a control IgG at the indicated concentrations. After two washes in cold medium, fresh ice-cold medium containing rLCMV-LASVGP (MOI, 10) in the presence of antibodies was added, and the cells were incubated on ice. At the indicated time points, unbound virus was removed by two rapid wash steps in cold medium, followed by addition of prewarmed medium and incubation at 37°C. At 4 h after the temperature shift, 20 mM ammonium chloride was added to prevent secondary infection. At a total of 16 h, the cells were fixed, and infection was detected by intracellular staining of LCMVNP.

For measurement of the viral entry kinetics, rLCMV-LASVGP and UUKV (MOI, 3) were added to cells on ice for 1 h. Unbound virus was removed by washing with cold medium. Prewarmed complete medium was added, and the cells were rapidly shifted to 37°C at 5% CO₂. Ammonium chloride (20 mM) was added at 0, 5, 10, 20, 40, 60, 120, and 240 min. After 7 (UUKV) or 16 (rLCMV-LASVGP) hours, infection was quantified by intracellular staining of the viral proteins by flow cytometry as described above.

Immunoblotting. Proteins were separated by SDS-PAGE and transferred to nitrocellulose. After blocking in 3% (wt/vol) skim milk in PBS, the membranes were incubated with 1 to 10 μ g/ml primary antibody in 3% (wt/vol) skim milk-PBS overnight at 4°C or 2 h at RT. After several washes in PBS-0.1% (wt/vol) Tween 20 (PBST), secondary antibodies coupled to HRP were applied at 1:6,000 in PBST for 1 h at room temperature. The blots were developed by enhanced chemiluminescence (ECL) using Super Signal West Pico ECL Substrate (Pierce).

Inhibitor studies in MDDC. MDDC were seeded in round-bottom 96-well plates (Costar) and pretreated for 30 min in the presence of sugars [mannan or GlcNAc β (1-2)Man] or anti-DC-SIGN antibodies (MAb

120507 or MAb DC28) on ice, for 2 h in the presence of chlorpromazine, or for 30 min in the presence of nocodazole; the actin inhibitors cytochalasin B, latrunculin A, and jasplakinoline; dynasore; ethylisopropyl amiloride (EIPA); and p21-activated kinase inhibitor III (IPA-3) at the indicated concentrations at 37°C. The cells were then infected in the presence of inhibitors for 1 h with rLCMV-LASVGP, UUKV, and rLCMV-VSVG at 37°C. At 4 h postinfection, 20 mM ammonium chloride was added to prevent secondary infection. Infection was detected after 7 (UUKV) or 16 (rLCMV-LASVGP) hours by flow cytometry as described above. The viability of drug-treated cells was determined by staining of single-cell preparations with LIVE/DEAD stain.

RESULTS

Upregulation of DC-SIGN in MDDC correlates with enhanced LASV entry. Previous studies demonstrated that primary MDDC are highly susceptible to infection with different LASV isolates and that productive infection causes virus-induced perturbation of their antigen-presenting function (5, 6). To investigate LASV entry into human DCs, we therefore used primary human MDDC as a model. Since LASV is a BSL4 pathogen, work with the live virus is restricted to laboratories with high security containment. To circumvent these biosafety concerns, we used a recombinant form of the genetically and structurally closely related prototypic arenavirus LCMV expressing the envelope GP of LASV (rLCMV-LASVGP) (36). The chimera rLCMV-LASVGP does not show significant attenuation *in vitro* compared to the parental LCMV strain and grows to robust titers. Since receptor binding and host cell entry of arenaviruses are mediated exclusively by the viral GP, rLCMV-LASVGP adopts the receptor binding characteristics of LASV. rLCMV-LASVGP has been used extensively to study LASV cell entry and cell tropism in cultured cells *in vitro* (36, 45, 46) and recently *in vivo* using a small-animal model (47). Notably, rLCMV-LASVGP showed marked tropism for DCs *in vitro* and *in vivo* and showed a tissue distribution reminiscent of that of LASV in human patients (47, 48). The rLCMV-LASVGP chimera therefore represents a powerful BSL2 surrogate for studies on LASV-receptor interaction and cell entry in the context of productive arenavirus infection.

In a first step, we evaluated productive infection of our rLCMV-LASVGP chimera in human MDDC. For this purpose, primary human monocytes were isolated from peripheral blood of healthy donors and differentiated *in vitro* in the presence of GM-CSF and IL-4, as described previously (5). Differentiation of monocytes into MDDC resulted in upregulation of DC-SIGN, as detected by flow cytometry and Western blotting (Fig. 1A and B). To assess susceptibility to rLCMV-LASVGP, monocytes and MDDC were infected at different multiplicities. The cells were fixed, and infection was detected by immunostaining for the intracellular viral nucleoprotein (NP) and quantification by flow cytometry. As a negative control, human CD4 T cells (Jurkat), which are refractory to LASV infection, were included. Compared to monocytes, MDDC showed increased susceptibility to rLCMV-LASVGP (Fig. 1C). In line with previous studies, CD4 T cells were highly resistant (Fig. 1C). Next, we determined virus production from infected monocytes and MDDC. Briefly, cells were infected with rLCMV-LASVGP at high multiplicity (3), and virus production was monitored by determination of infectious viral titers in the cell supernatants over time using an IFA. Compared to monocytes, MDDC produced >10-fold-larger amounts of infectious virus (Fig. 1D). The increased susceptibility to rLCMV-LASVGP of MDDC compared to monocytes closely resembled previous

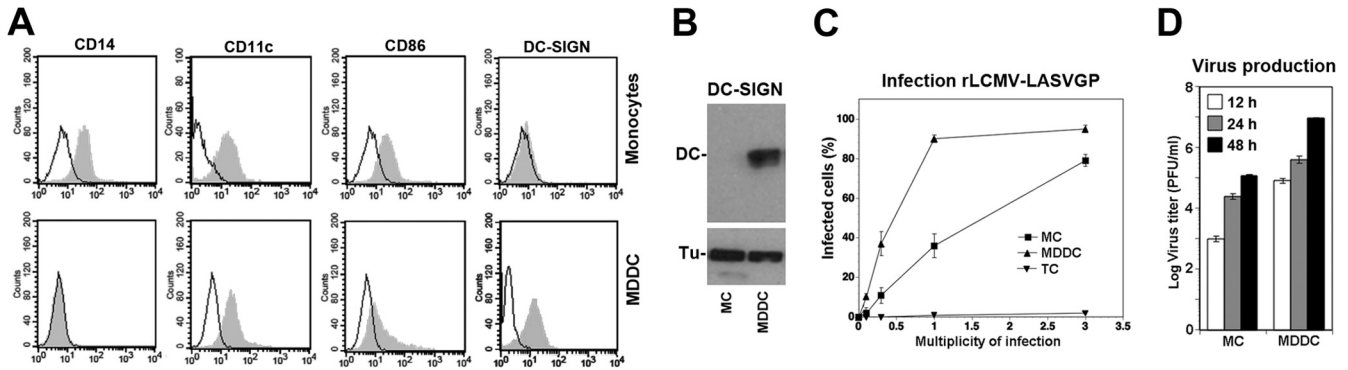


FIG 1 Infection of MDDC by rLCMV-LASVGP. (A) Primary human monocytes were isolated from peripheral blood of healthy donors and differentiated in the presence of GM-CSF and IL-4, as described in Materials and Methods. The indicated markers were detected by immunostaining on live, nonpermeabilized cells and analyzed by flow cytometry, as described in Materials and Methods. Empty peaks, secondary antibody only; shaded peaks, primary and secondary antibodies. One representative example is shown out of three experiments with different donors. (B) Detection of DC-SIGN in monocytes and MDDC. Monocytes (MC) and MDDC differentiated as in panel A were lysed, and total proteins were separated by SDS-PAGE and blotted to nitrocellulose. The blots were probed with MAb 120507 to DC-SIGN and an HRP-conjugated secondary antibody using ECL for development. As a loading control, α -tubulin was detected. The positions of DC-SIGN (DC) and α -tubulin (Tu) are indicated. One representative example is shown out of two experiments with different donors. (C) Infection of monocytes and MDDC with rLCMV-LASVGP. Primary human blood monocytes were either kept as MC or differentiated into MDDC. As a control, Jurkat cells (TC) were used. The cells were infected with rLCMV-LASVGP at the indicated MOIs. After 24 h, the cells were fixed, and infection was detected by intracellular staining of LCMVNP in flow cytometry. The results are means \pm standard deviations (SD) ($n = 3$). For monocytes and MDDC, three different donors were used. (D) Virus production. MC and MDDC were infected with rLCMV-LASVGP at a high MOI of 3. At the indicated time points, supernatants were collected and infectious virus titers were determined by IFA on monolayers of VeroE6 cells. The data are means \pm SD of three experiments with different donors.

observations made with live LASV isolates (5) and correlated with the strong upregulation of DC-SIGN. Recent studies showed the absence of the TAM kinases Axl and Dtk from MDDC (33). We confirmed these previous findings by probing TAM receptor expression in monocytes and MDDC by flow cytometry (Fig. 2) and Western blotting (data not shown). While primary human monocytes express low levels of Dtk, none of the TAM receptors was detected in MDDC.

LASVGP binds DC-SIGN via mannose glycans on the receptor binding GP1. Considering the correlation between DC-SIGN expression and susceptibility to rLCMV-LASVGP infection in monocytes versus MDDC, DC-SIGN represented an interesting candidate LASV receptor in MDDC. To further characterize the

molecular interaction between LASVGP and DC-SIGN, we used the authentic inactivated LASV strain Josiah, provided by the Special Pathogens Branch of the Centers for Disease Control and Prevention. To define the part of LASVGP involved in DC-SIGN binding, we first addressed the relative contributions of the N-terminal GP1 and the transmembrane GP2. For this purpose, the virus was immobilized in microtiter plates and treated with 1 M NaCl, which results in complete dissociation of GP1 from virions but does not affect GP2 (49). Virus stripped with high levels of salt and untreated control virus were incubated with C-terminal fusion proteins of recombinant DG, known to bind GP1, and DC-SIGN with human IgG Fc (DG-Fc and DC-SIGN-Fc). Virus-bound DG-Fc and DC-SIGN-Fc were then detected with an HRP-

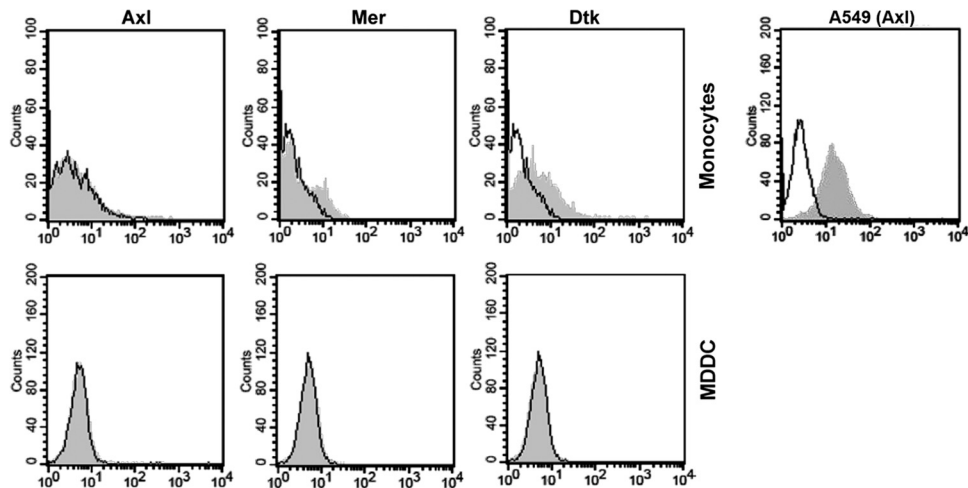


FIG 2 MDDC lack the TAM receptors Axl, Dtk, and Mer. Live, nonpermeabilized monocytes and MDDC were stained for the TAM receptors Axl, Dtk, and Mer with specific antibodies, followed by fixation, detection with PE-conjugated secondary antibodies, and analysis by flow cytometry. As a positive control for Axl, A549 cells were included. Empty peaks, secondary antibody only; shaded peaks, primary and secondary antibodies. One representative example is shown out of three experiments with different donors.

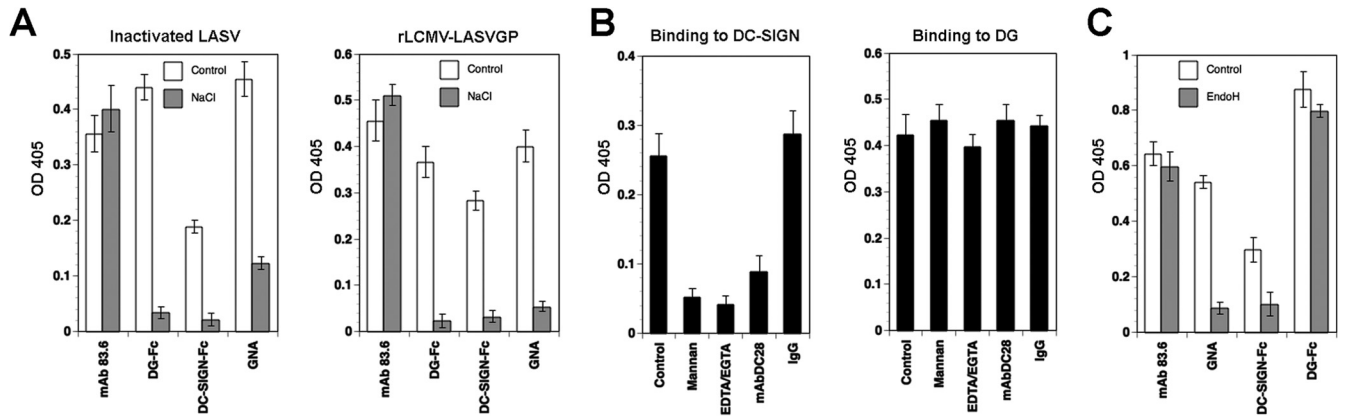


FIG 3 Characterization of the interaction of LASVGP with DC-SIGN. (A) DC-SIGN binds to LASV GP1. Inactivated LASV and rLCMV-LASVGP purified over a Renografin gradient were immobilized in microtiter plates and treated with 1 M NaCl for 1 h (NaCl) or left in PBS (Control). After several washes in PBS, recombinant DC-SIGN-Fc, DG-Fc, MAb 83.6 to LASV GP2, and biotinylated GNA were added. Bound Fc fusion proteins were detected with HRP-conjugated anti-human IgG Fc, MAb 83.6 with an HRP-conjugated anti-mouse IgG, and GNA with HRP-linked streptavidin in a color reaction. The data represent OD values with background subtraction (means \pm SD; $n = 3$). (B) Binding of DC-SIGN to rLCMV-LASVGP is blocked by mannan, EDTA/EGTA, and MAb DC28. DC-SIGN-Fc (left) and DG-Fc (right) were immobilized in microtiter plates and treated with mannan (25 μ g/ml), 5 mM EDTA/EGTA, 20 μ g/ml MAb DC28, and IgG isotype control (IgG) at 20 μ g/ml for 1 h. Purified rLCMV-LASVGP was added at 10^7 PFU/ml in the presence of inhibitors for 2 h in the cold. Bound virus was detected with MAb 83.6 to LASV GP2, combined with an HRP-conjugated secondary antibody in a color reaction as for panel A (means \pm SD; $n = 3$). (C) Removal of mannose sugars from LASVGP reduces binding to DC-SIGN. rLCMV-LASVGP was immobilized and subjected to treatment with EndoH glycosidase for 12 h at room temperature (EndoH) or left untreated (Control). After several washes, binding to DC-SIGN-Fc, DG-Fc, GNA, and MAb 83.6 was assessed as for panel A (means \pm SD; $n = 3$).

conjugated secondary antibody in a color reaction. The presence of mannose glycans in the viral glycoproteins was detected with the lectin *Galanthus nivalis* agglutinin (GNA), which specifically binds to α (1-3)-linked mannose. To monitor possible detachment of virus due to high-salt treatment, the membrane-associated GP2 was detected with MAb 83.6. High-salt treatment of inactivated LASV markedly reduced binding of DG-Fc, DC-SIGN-Fc, and the mannose-specific lectin GNA, whereas the signal for GP2 was unaffected (Fig. 3A). The results indicate that DC-SIGN binds to LASV GP1, which bears mannose glycans. The very similar DC-SIGN binding characteristics observed with authentic LASV and rLCMV-LASVGP further confirmed that our chimera virus is an adequate model to study LASV-DC-SIGN interactions.

The binding of DC-SIGN to mannose-rich glycans present on pathogens critically depends on divalent cations and can be blocked by the sugar polymer mannan and MAb DC28 to DC-SIGN (20, 22, 23, 25, 28). To assess the effects of these inhibitors on the interaction between LASV GP1 and DC-SIGN, DC-SIGN-Fc was immobilized and pretreated with mannan, EDTA/EGTA, and MAb DC28 to DC-SIGN (Fig. 3B), suggesting a role of LASV GP1-derived mannose sugars in recognition of DC-SIGN. To corroborate a role of LASV GP1-linked mannose sugars in DC-SIGN binding, immobilized rLCMV-LASVGP was treated with EndoH, which specifically removes high-mannose *N*-glycans, but not hybrid and complex *N*-glycans. Subsequent probing with DC-SIGN-Fc and GNA revealed a significant reduction of binding, whereas attachment of DG-Fc and MAb 83.6 to GP2 was unaf-

ected (Fig. 3C). Taken together, our data reveal that LASVGP binds to DC-SIGN via mannose glycans on GP1.

DC-SIGN mediates attachment of rLCMV-LASVGP to MDDC. In the next step, we addressed a possible role of DC-SIGN in attachment of LASV to human DCs. For this purpose, we performed a well-established virus-cell binding assay that had been previously used to characterize cellular receptors for LCMV (11, 44). Briefly, rLCMV-LASVGP was purified over a Renografin gradient and labeled with biotin using the reagent NHS-X-biotin. Biotinylated virus was tested for infectivity, and only preparations that retained $>50\%$ infectious-virus titers were used for further experimentation. Monocytes, MDDC, and CD4 T cells were incubated with biotinylated virus at increasing particle/cell ratios in the cold. Unbound virus was removed by washing, and the cells were fixed. Bound virions were detected with streptavidin conjugated to Alexa 488 in flow cytometry. The binding curves displayed in Fig. 4A revealed a marked increase in virus binding to MDDC compared to monocytes, consistent with the enhanced susceptibility to productive infection (Fig. 1C). As expected, CD4 T cells showed negligible virus binding. To address the role of DC-SIGN in virus attachment to MDDC, cells were pretreated with mannan and MAb DC28 prior to exposure to biotin-labeled virus. Treatment with both mannan and MAb DC28 resulted in a dose-dependent reduction of virus binding to MDDC (Fig. 4B), implicating DC-SIGN in virus attachment. To complement these studies, labeled virus was pretreated with DC-SIGN-Fc, followed by binding to MDDC. Exposure of virus to DC-SIGN-Fc, but not an isotype Fc control, resulted in a dose-dependent reduction of virus binding (Fig. 4C). Together, the data indicate a role for DC-SIGN in attachment of free virus to MDDC.

DC-SIGN facilitates productive infection of rLCMV-LASVGP in MDDC. The apparent role of DC-SIGN in attachment of rLCMV-LASVGP to MDDC (Fig. 4) raised the possibility that DC-SIGN could function as an entry receptor for LASV, sim-

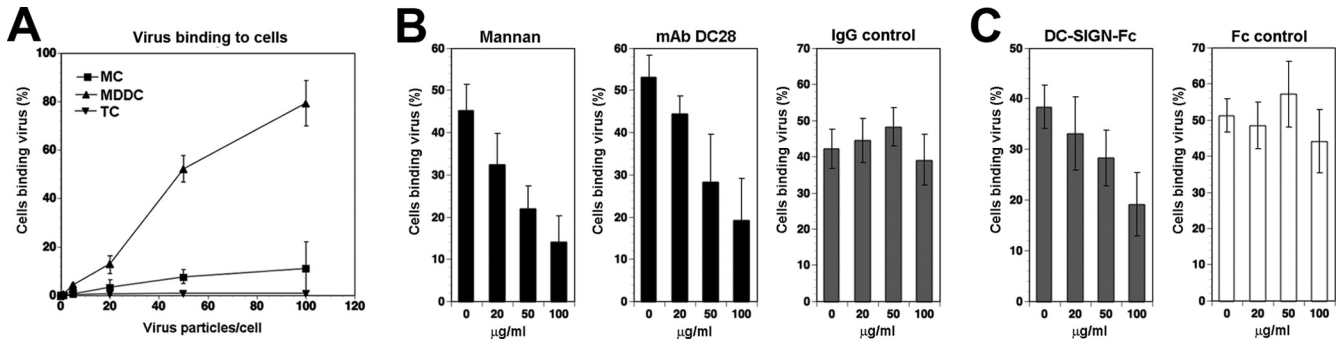


FIG 4 DC-SIGN is an attachment factor for rLCMV-LASVGP in MDDC. (A) Binding of rLCMV-LASVGP to monocytes and MDDC. Biotinylated rLCMV-LASVGP was added to monocytes, MDDC, and Jurkat cells at the indicated particle/cell ratios for 1 h at 4°C. Unbound virus was removed, the cells were fixed, and bound virus was detected with streptavidin labeled with Alexa 488. Virus-binding cells were detected by flow cytometry. The data are means \pm SD of three experiments with different donors. (B) Blocking of virus binding to MDDC. MDDC were treated with the indicated concentrations of mannan, MAb DC28 to DC-SIGN, and control IgG for 2 h on ice, followed by incubation with biotinylated rLCMV-LASVGP at 50 particles/cell for 1 h in the cold. Bound virus was detected as for panel A, and the percentages of virus-binding cells are displayed. The data are means \pm SD of three experiments with different donors. (C) Blocking of virus binding with DC-SIGN-Fc. Biotinylated rLCMV-LASVGP was incubated with the indicated concentrations of DC-SIGN-Fc and Fc control for 2 h on ice and then added to MDDC for 1 h in the cold. Virus-binding cells were assessed as for panel A. The results are means \pm SD of three experiments with different donors.

ilar to what has been observed for the phleboviruses UUKV and RVFV (28). In the next step, we therefore compared the roles of DC-SIGN in productive infection of rLCMV-LASVGP and UUKV in MDDC. In a first step, cells were pretreated with the DC-SIGN ligand mannan, followed by infection with rLCMV-LASVGP and UUKV in the presence of the inhibitor. At 4 h postinfection, 20 mM ammonium chloride was added to avoid secondary infection. Infected cells were detected by intracellular

staining for LCMVNP and UUKV antigen in flow cytometry after 16 and 7 h, respectively. Blocking with mannan resulted in only mild reduction (<30%) of infection with rLCMV-LASVGP, whereas UUKV infection was diminished by >90% (Fig. 5A). To more specifically block DC-SIGN-mediated infection, MDDC were pretreated with MABs DC28 and 120507 to DC-SIGN prior to and during infection with rLCMV-LASVGP and UUKV. Pretreatment of MDDC with MABs DC28 and 120507 reduced infec-

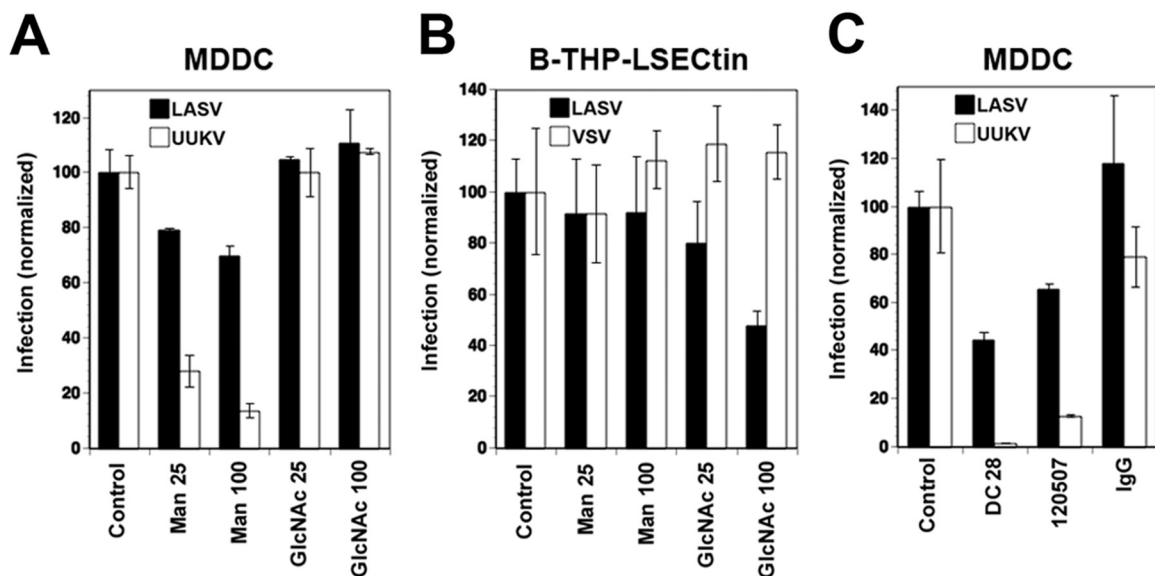


FIG 5 DC-SIGN facilitates cell entry of rLCMV-LASVGP. (A) Blocking of virus infection in MDDC. MDDC were treated with 25 μ g/ml mannan (Man 25), 100 μ g/ml mannan (Man 100), 25 μ g/ml GlcNAc β (1-2)Man (GlcNAc 25), 100 μ g/ml GlcNAc β (1-2)Man (GlcNAc 100), and PBS vehicle control (Control) for 30 min at 37°C. The cells were then infected with rLCMV-LASVGP (LASV) and UUKV at an MOI of 3 for 1 h in the presence of inhibitors. The cells were washed, and at 4 h postinfection, 20 mM ammonium chloride was added to prevent secondary infection. Infection was assessed by FACS. Infection was normalized by setting control specimens at 100%. The data are means \pm SD of three experiments with different donors (6 donors in total). (B) B-THP-LSECTin cells were treated with inhibitors as for panel A, followed by infection with rLCMV-LASVGP (LASV) and rLCMV-VSVG (VSV) at an MOI of 10. Infection was assessed by IFA after 16 h, and the data were normalized as for panel A. (C) Blocking of virus infection in MDDC with MAB to DC-SIGN. MDDC were treated with 20 μ g/ml of MAB DC28 (DC28), MAB 120507 (120507), isotype control IgG (IgG), or PBS (Control) for 30 min at 37°C, followed by infection with rLCMV-LASVGP and UUKV as for panel A. Infection was normalized by setting control specimens at 100%. The data are means \pm SD of two experiments with different donors (4 donors in total).

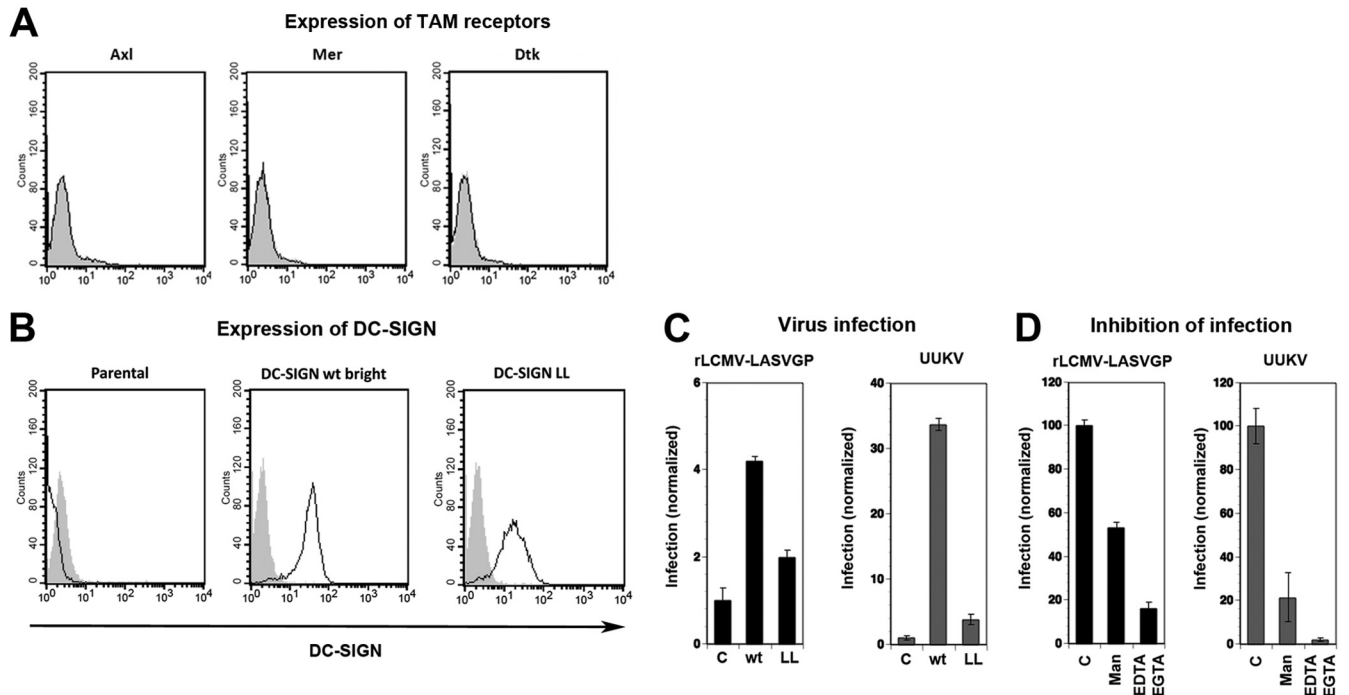


FIG 6 Different efficiencies of DC-SIGN in cell entry of rLCMV-LASVGP and UUKV. (A) Detection of TAM receptors in parental Raji cells by flow cytometry as in Fig. 2. Empty peaks, secondary antibody only; shaded peaks: primary and secondary antibodies. (B) Detection of DC-SIGN in Raji cell lines. Raji parental cells, Raji-DC-SIGN, and Raji-DC-SIGN-LL cells were stained with MAb 120507 to DC-SIGN combined with a PE-conjugated secondary antibody and analyzed by flow cytometry. Empty peaks, primary and secondary antibodies; shaded peaks, secondary antibody only. (C) Virus infection of Raji cell lines. Raji parental cells (C), Raji-DC-SIGN cells (wt), and Raji-DC-SIGN-LL cells (LL) were infected with rLCMV-LASVGP and UUKV at an MOI of 3. At 4 h postinfection, 20 mM ammonium chloride was added to avoid secondary infection. Infection was assessed by intracellular staining for LCMVNP and UUKV antigen, respectively, and infected cells were detected by flow cytometry (means \pm SEM; $n = 2$). (D) Inhibition of infection of Raji-DC-SIGN cells. Raji-DC-SIGN cells were treated with 50 μ g/ml mannan (Man), 5 mM EDTA/EGTA, or PBS vehicle control (C) for 30 min, followed by infection with rLCMV-LASVGP and UUKV. Infection was assessed as for panel B and normalized by setting control specimens at 100% (means \pm SEM; $n = 2$).

tion with rLCMV-LASVGP by circa 60% and 40%, respectively. In contrast, infection with UUKV was consistently reduced by >90% (Fig. 5C). The only partial blocking of rLCMV-LASVGP infection in MDDC by anti-DC-SIGN antibodies suggested that DC-SIGN somehow facilitated viral entry and productive infection but was not strictly required.

Another candidate receptor identified for LASV is the C-type lectin LSEctin, identified in a recent expression-cloning approach (16). Since LSEctin can be present on MDDC under some conditions (50), we addressed a potential role of LSEctin in LASV entry into MDDC. For this purpose, cells were pretreated with increasing concentrations of the LSEctin ligand GlcNAc β (1-2)Man, followed by infection with rLCMV-LASVGP and UUKV. Treatment of MDDC with up to 100 μ g/ml GlcNAc β (1-2)Man did not affect infection with the two viruses (Fig. 5A). To confirm the efficiency of our inhibitor treatment, we used B-THP-1 cells expressing recombinant LSEctin (35). In line with previous studies (16), pretreatment with 100 μ g/ml GlcNAc β (1-2)Man, but not mannan, significantly reduced infection with rLCMV-LASVGP. As a negative control, we included a recombinant LCMV expressing the G protein of vesicular stomatitis virus (rLCMV-VSVG), which is not dependent on LSEctin and was not affected by the inhibitor treatment (Fig. 5B). Together, our data make a major contribution of LSEctin to the entry of rLCMV-LASVGP in MDDC appear unlikely.

Different efficiencies of DC-SIGN in mediating entry of rLCMV-LASVGP and UUKV. The data at hand indicated that

DC-SIGN can facilitate attachment and entry of rLCMV-LASVGP in MDDC. In contrast, UUKV, RVFV, and other bunyaviruses can use DC-SIGN alone for binding and infectious uptake, suggesting different roles of DC-SIGN in entry. To assess the relative efficiencies of DC-SIGN in mediating productive infection by rLCMV-LASVGP and UUKV, we utilized Raji cells stably transfected with wild-type DC-SIGN and a DC-SIGN mutant containing a mutation in the cytoplasmic LL motif that is impaired in endocytosis (34). Parental Raji cells lacked TAM receptors (Fig. 6A) and expressed only negligible levels of DC-SIGN (Fig. 6B), making them refractory to rLCMV-LASVGP and UUKV. The Raji-DC-SIGN and Raji-DC-SIGN-LL stable transfectants expressed similar amounts of DC-SIGN on their surfaces (Fig. 6B). Parental Raji cells, Raji-DC-SIGN, and Raji-DC-SIGN-LL were infected with rLCMV-LASVGP and UUKV. Productive infection was assessed after one round of replication and normalized to the untransfected parental line. In line with previous studies, expression of DC-SIGN increased infection with UUKV by >40-fold (28), whereas only circa 4-fold enhancement of rLCMV-LASVGP infection was observed (Fig. 6C). Compared to wild-type DC-SIGN, DC-SIGN-LL was less efficient in mediating infection with rLCMV-LASVGP and UUKV (Fig. 6C). Infection of rLCMV-LASVGP and UUKV in Raji-DC-SIGN cells was blocked upon treatment with mannan and the chelators EDTA/EGTA (Fig. 5C), confirming a role of DC-SIGN in enhancement of infection. The data obtained with Raji cells expressing recombinant DC-SIGN

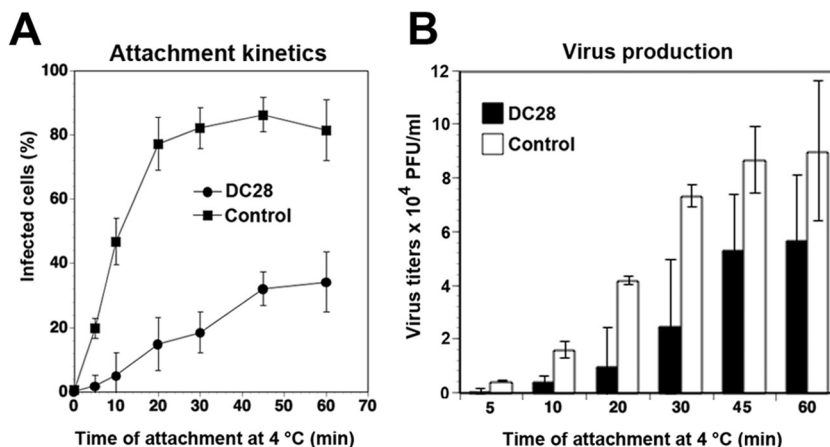


FIG 7 Attachment and entry kinetics of rLCMV-LASVGP in MDDC. (A) DC-SIGN accelerates the capture of free virus. MDDC were pretreated with MAb DC28 to DC-SIGN and control IgG (Control) for 1 h in the cold, followed by binding of rLCMV-LASVGP at an MOI of 10. At the indicated time points, unbound virus was removed by washing, and the cells were shifted to 37°C. Productive infection was detected after a total of 16 h by FACS (means \pm SEM; $n = 3$). (B) Conditioned cell culture supernatants from panel A were assessed for infectious-virus titers by IFA as for Fig. 1D. The data are means \pm SD of three experiments with different donors.

are in line with our findings in MDDC (Fig. 7). The fact that rLCMV-LASVGP and UUKV present significant differences in their abilities to infect DC-SIGN⁺ cells may reflect distinct roles of the lectin in mediating cell entry of these viruses.

DC-SIGN accelerates the capture of free rLCMV-LASVGP by MDDC. A hallmark of lectin-type carbohydrate-protein interactions is their relatively high on-rates, opening the possibility that DC-SIGN may be involved in the capture of free rLCMV-LASVGP by human DCs. To address this possibility, we investigated the role of DC-SIGN in the attachment kinetics of rLCMV-LASVGP in MDDC. Cells were chilled on ice and preincubated with MAb CD28 to DC-SIGN or a control IgG in the cold. rLCMV-LASVGP was then added at an MOI of 10 in the presence of the antibodies. At the indicated time points, unbound virus was removed by washing, and the cells were rapidly shifted to 37°C. After 4 h, ammonium chloride was added, and infection was detected after 16 h by flow cytometry. In the presence of control IgG, the virus rapidly attached to cells and reached saturation with half-maximal binding after <15 min (Fig. 7A). Blocking of DC-SIGN with MAb DC28 resulted in slower virus attachment that hardly reached saturation after 45 min. After <45 min of attachment, we noticed reduced viral titers produced from cells treated with anti-DC-SIGN antibody (Fig. 7B). The data suggest that DC-SIGN can accelerate capture of free virus, facilitating productive infection.

rLCMV-LASVGP enters MDDC via a slow actin-dependent pathway. The apparently different roles of DC-SIGN in productive infection by rLCMV-LASVGP and UUKV raised the possibility that the viruses may use distinct pathways for cell entry. In a first step, we compared the entry kinetics of rLCMV-LASVGP and UUKV in MDDC. Both viruses require a pH of <6.0 for fusion, indicating delivery to late endosomes for productive cell entry (28, 45). To assess how fast receptor-bound rLCMV-LASVGP and UUKV trafficked to late endosomes, we determined the time required for the viruses to become resistant to ammonium chloride. When added to cells, ammonium chloride raises the endosomal pH rapidly and blocks low-pH-dependent membrane fusion without causing overall cytotoxicity (51, 52). The viruses were

bound to MDDC in the cold, allowing receptor attachment without internalization. Unbound virus was removed, and the cells were shifted to 37°C to restore membrane movements. Ammonium chloride was added at different time points postinfection and kept throughout the experiment. Cells were fixed, and infection was assessed by flow cytometry. In line with published data, 50% of UUKV had escaped from the late endosome after circa 20 min (28). In contrast, cell entry of rLCMV-LASVGP was markedly slower, with <50% of the virus having escaped from the endosome after 1 h (Fig. 8A).

To test the involvement of actin-dependent pathways, like macropinocytosis or phagocytosis, that are present in MDDC, we treated cells with cytochalasin D or latrunculin A, which disrupt actin fibers, as well as jasplakinolide, an actin-polymer-stabilizing drug that blocks the dynamics of actin filaments. When added to cells for 30 min prior to infection, cytochalasin D, latrunculin A, and jasplakinolide significantly reduced infection by rLCMV-LASVGP, but not UUKV (Fig. 8B). Previous studies revealed that UUKV associates in MDDC with clathrin-coated pits (28). A possible role of clathrin-mediated endocytosis (CME) in the entry of rLCMV-LASVGP into MDDC was therefore addressed using chlorpromazine (CPZ), a drug that perturbs the assembly of clathrin-coated pits at the plasma membrane. As a positive control, we included a recombinant VSV pseudotype that contains a GFP reporter and bears VSVG (rVSV Δ G*-VSVG) in its envelope, which mediates cell entry in a clathrin- and dynamin-dependent manner (53). The VSV pseudotype lacks endogenous G and is limited to one round of replication, limiting viral spread. Treatment of MDDC with up to 8 μ M CPZ did not significantly affect infection with rLCMV-LASVGP but reduced infection of rVSV Δ G*-VSVG in a dose-dependent manner (Fig. 8C). To address the involvement of dynamin in rLCMV-LASVGP cell entry, MDDC were treated with the dynamin inhibitor dynasore prior to infection. As a control, we again included rVSV Δ G*-VSVG. As shown in Fig. 8D, infection of MDDC with rLCMV-LASVGP was not affected by up to 100 μ M dynasore, whereas infection with rVSV Δ G*-VSVG was reduced.

The actin dependence and apparent clathrin and dynamin in-

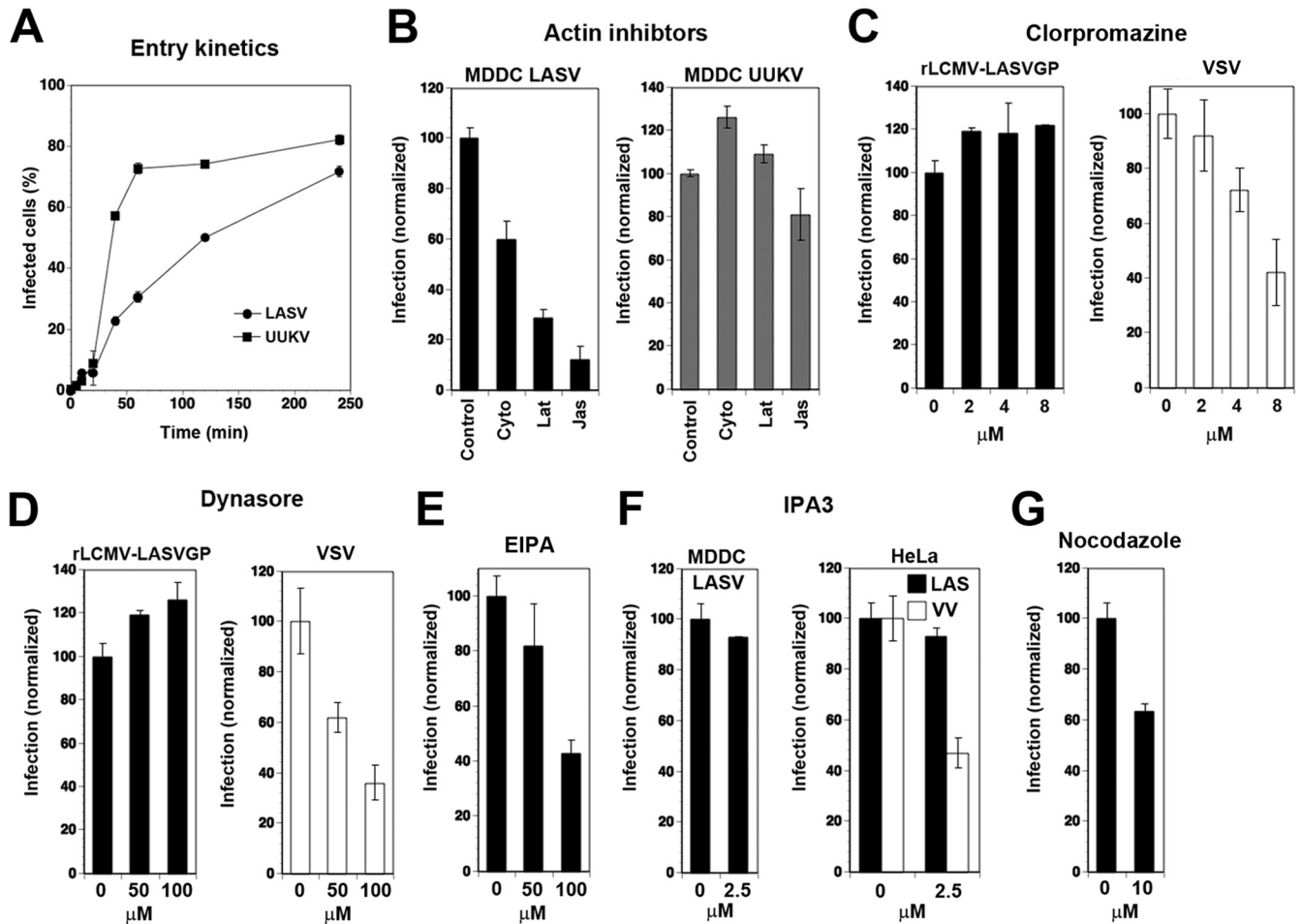


FIG 8 Characterization of rLCMV-LASVGP entry into MDDC. (A) Entry kinetics of rLCMV-LASVGP and UUKV in MDDC. MDDC were incubated with rLCMV-LASVGP and UUKV at an MOI of 3 for 1 h in the cold. Unbound virus was removed, and the cells were shifted to 37°C. At the indicated time points, 20 mM ammonium chloride was added and left throughout the experiment. After 16 h (rLCMV-LASVGP) and 7 h (UUKV), the cells were fixed, and infection was detected as for Fig. 6. The percentage of infected cells was plotted against time; the data are means \pm SEM of three experiments with three different donors. (B) Infection of rLCMV-LASVGP in MDDC is actin dependent. MDDC were treated with 20 μ M cytochalasin D (Cyto), 5 μ M latrunculin A (Lat), and 1 μ M jasplakinolide (Jas) or with solvent control (Control) for 30 min, followed by infection with rLCMV-LASVGP and UUKV as for panel A. The data are means \pm SD of three experiments with three different donors. (C) Effect of CPZ on infection with rLCMV-LASVGP. MDDC were treated with the indicated concentrations of CPZ or PBS only (0) for 1 h, followed by infection with rLCMV-LASVGP or rVSV Δ G⁺-VSVG (VSV) at an MOI of 10. After 4 h, 20 mM ammonium chloride was added to prevent secondary infection, and rLCMV-LASVGP-infected cells were detected after 16 h as for panel A. Cells infected with rVSV Δ G⁺-VSVG were fixed after 6 h, and GFP was detected by direct fluorescence. At 6 h postinfection, MDDC infected with rVSV Δ G⁺-VSVG, but not rLCMV-LASVGP, started to show signs of activation. Infection was normalized by setting untreated specimens at 100%. The data are means \pm SD of three experiments with three different donors. (D) Blocking of infection by rLCMV-LASVGP with dynasore. MDDC were pretreated with the indicated concentrations of dynasore or vehicle control (0), followed by infection with rLCMV-LASVGP or rVSV Δ G⁺-VSVG (VSV) as for panel C. The data are means \pm SD of three experiments with three different donors. (E) Inhibition of rLCMV-LASVGP infection in MDDC by EIPA. MDDC were pretreated with the indicated concentrations of EIPA or vehicle control (0) for 30 min prior to infection with rLCMV-LASVGP as for panel B. The data are means and SD of three experiments with three different donors. (F) Effect of the PAK1 inhibitor IPA-3 on infection with rLCMV-LASVGP. MDDC and HeLa cells were pretreated with the indicated concentration of IPA-1 or vehicle control (0) for 30 min, followed by infection with rLCMV-LASVGP (LASV) or recombinant vaccinia virus expressing GFP (VV). Infection with rLCMV-LASVGP was assessed as for panel B and infection with VV by detection of the GFP reporter in direct-fluorescence microscopy at 12 h postinfection. The data are means \pm SD of three experiments with three different donors. (G) Role of microtubules in rLCMV-LASVGP infection in MDDC. MDDC were pretreated with nocodazole (10 μ M) or solvent control (0), and infection with rLCMV-LASVGP was performed as for panel B. The data are means and SD of three experiments with three different donors.

dependence of rLCMV-LASVGP cell entry into MDDC suggested a possible role of macropinocytosis in the process (54). Treatment of cells with the Na⁺/H⁺ exchanger inhibitor EIPA reduced infection with rLCMV-LASVGP, but only at relatively high concentrations (Fig. 8E). We further used the PAK1 inhibitor IPA-3, which plays a central role in macropinocytosis of some viruses, e.g., vaccinia virus (55). As shown in Fig. 8F, IPA-3 had no significant effect on infection by rLCMV-LASVGP in MDDC

but reduced infection of HeLa cells with vaccinia virus, in line with published data (55). Since vesicular transport to late endosomes in many cell types depends on microtubules (56), we tested the effect of nocodazole, a drug that dissociates microtubular structures, on rLCMV-LASVGP entry into MDDC. Pretreatment of cells with nocodazole reduced infection with rLCMV-LASVGP to some extent, indicating a role of microtubules in the process (Fig. 8G).

DISCUSSION

Here, we studied the role of the C-type lectin DC-SIGN in entry of LASV into human MDDC using a recombinant LCMV expressing LASVGP (rLCMV-LASVGP) as a BSL2 surrogate for LASV. We found that differentiation of primary human monocytes into MDDC enhanced susceptibility to rLCMV-LASVGP infection, a situation similar to the one observed with live LASV isolates (5). The upregulation of DC-SIGN in MDDC correlated with markedly stronger virus attachment and enhanced productive infection, suggesting a role of DC-SIGN in attachment and/or infection of rLCMV-LASVGP, similar to its function in cell entry of the arthropod-borne phleboviruses UUKV and RVFV (28).

Previous studies on the role of DC-SIGN in entry of UUKV and RVFV showed that these viruses bind to DC-SIGN via high-mannose *N*-glycans present on their glycoproteins (28). Our present studies revealed a similar binding mechanism for LASV involving *N*-linked mannose sugars on GP1, in line with the previously reported observation that LASV GP1 contains a high proportion of mannose sugars (57), similar to the glycoproteins of arthropod-borne viruses. To investigate the role of DC-SIGN in different steps of LASV cell entry, we first performed virus-cell binding assays and found that DC-SIGN is involved in attachment of the virus to MDDC. To address the function of DC-SIGN in productive infection, we compared rLCMV-LASVGP with UUKV, which uses DC-SIGN as an authentic entry receptor (28). Blocking of DC-SIGN on MDDC with mannan and antibodies almost completely abolished UUKV infection but only partially reduced infection with rLCMV-LASVGP. Using Raji cells stably expressing DC-SIGN, we confirmed the different efficiencies of DC-SIGN in mediating infection with rLCMV-LASVGP and UUKV. While recombinant DC-SIGN greatly enhanced productive infection with UUKV, as shown previously (28), the effect on rLCMV-LASVGP was more modest.

The data at hand supported a role of DC-SIGN as an entry factor for rLCMV-LASVGP, raising the question about the possible physiological relevance of the LASV–DC-SIGN interaction. In early LASV infection, the virus infects DCs at the site of inoculation, and the kinetics of free-virus capture by DCs may therefore be an important determinant of efficient productive infection. To address the role of DC-SIGN in virus capture by MDDC, we determined the kinetics of virus-cell attachment in the presence and absence of function-blocking anti-DC-SIGN antibodies. Using productive infection as a readout, we provide the first evidence that DC-SIGN can accelerate the capture of free virus by MDDC.

The data at hand suggested that DC-SIGN can facilitate LASV infection of MDDC at the level of virus-cell attachment. However, its role in the subsequent cell entry process was unclear. UUKV and LASV require similarly low pHs for fusion, indicating that both viruses escape from late endosomal compartments (31, 58, 59). Previous live-cell microscopy studies performed with UUKV revealed that, upon virus attachment, the virus–DC-SIGN complex is rapidly internalized and delivered to early endosomes, followed by transport of the virus to the late endosome, where fusion occurs after only 9 to 15 min (28). Monitoring of viral entry kinetics in MDDC revealed that UUKV escaped from the endosome with a half-time of less than 20 min, whereas <50% of rLCMV-LASVGP had escaped after 1 h. Using a combination of actin inhibitors, we found that entry of rLCMV-LASVGP, but not UUKV, was actin dependent. In contrast to UUKV, which associ-

ated with clathrin-coated pits in MDDC (28), studies with inhibitors provided the first evidence that entry of rLCMV-LASVGP was independent of clathrin and dynamin. The strong actin dependence of rLCMV-LASVGP entry into MDDC and its sensitivity to the amiloride EIPA, a potent inhibitor of the Na/H⁺ exchanger, rather suggest an entry pathway related to macropinocytosis that is constitutively active in MDDC. The distinct entry pathways used, together with the substantial DC-SIGN-independent infection of rLCMV-LASVGP, suggest roles of DC-SIGN in cell entry of LASV rather different from those of phleboviruses like UUKV and RVFV. In contrast to phleboviruses that use DC-SIGN as an entry receptor, DC-SIGN seems to serve primarily as an attachment factor for LASV in MDDC involved in virus capture. The partial independence of rLCMV-LASV entry from DC-SIGN suggests the existence of additional LASV entry factors in MDDC. Of particular importance in this context is the role of DG, which represents a major LASV receptor. LASV binding to DG critically depends on functional glycosylation of the receptor, in particular, specific O-linked glycans present on α -DG synthesized by the glycosyltransferase LARGE that are also crucial for recognition of DG's ECM ligands (32, 60). While the core protein of DG is ubiquitously expressed, the functional glycosylation of the receptor is under tight tissue-specific control (61). In previous studies, we found that many human cell types targeted *in vivo* by LASV, such as epithelial cells, vascular endothelial cells, and hepatocytes, express functionally glycosylated DG able to bind LASV with high affinity (62). However, the functional glycosylation of DG in human DCs, including MDDC, is currently unknown. Our initial attempts to detect functional DG in primary human MDDC in this study gave unclear results, suggesting possible differences in the extent or nature, or both, of functional glycosylation of DG compared to other cell types. In-depth characterization of the posttranslational modification of DG in human DCs, and its possible role as an entry factor for LASV, is under way in our laboratory and will contribute to a better understanding of LASV entry into this pivotal cell type

ACKNOWLEDGMENTS

We thank Stefan Pöhlmann (Deutsches Primatenzentrum, Göttingen, Germany) for providing us with the B-THP-1 cell line expressing LSECtin. We acknowledge Christelle Pythoud, Jillian M. Rojek, and Laetitia Basterra for their contributions to these studies. The antibody IIH6 to dystroglycan was provided by Kevin P. Campbell, Howard Hughes Medical Institute, University of Iowa.

This research was supported by Swiss National Science Foundation grant FN 310030_132844 (S.K.).

REFERENCES

- McCormick JB, Fisher-Hoch SP. 2002. Lassa fever. *Curr. Top. Microbiol. Immunol.* 262:75–109.
- McCormick JB, King IJ, Webb PA, Scribner CL, Craven RB, Johnson KM, Elliott LH, Belmont-Williams R. 1986. Lassa fever. Effective therapy with ribavirin. *N. Engl. J. Med.* 314:20–26.
- Johnson KM, McCormick JB, Webb PA, Smith ES, Elliott LH, King IJ. 1987. Clinical virology of Lassa fever in hospitalized patients. *J. Infect. Dis.* 155:456–464.
- Geisbert TW, Jahrling PB. 2004. Exotic emerging viral diseases: progress and challenges. *Nat. Med.* 10:S110–S121.
- Baize S, Kaplon J, Faure C, Pannetier D, Georges-Courbot MC, Deubel V. 2004. Lassa virus infection of human dendritic cells and macrophages is productive but fails to activate cells. *J. Immunol.* 172:2861–2869.
- Mahanty S, Hutchinson K, Agarwal S, McRae M, Rollin PE, Pulendran B. 2003. Cutting edge: impairment of dendritic cells and adaptive immunity by Ebola and Lassa viruses. *J. Immunol.* 170:2797–2801.
- Buchmeier MJ, de la Torre JC, Peters CJ. 2007. Arenaviridae: the viruses

- and their replication, p 1791–1828. *In* Knipe DL, Howley PM (ed), *Fields virology*, 4th ed. Lippincott-Raven, Philadelphia, PA.
8. de la Torre JC. 2009. Molecular and cell biology of the prototypic arenavirus LCMV: implications for understanding and combating hemorrhagic fever arenaviruses. *Ann. N. Y. Acad. Sci.* 1171(Suppl. 1):E57–E64.
 9. Meyer BJ, de La Torre JC, Southern PJ. 2002. Arenaviruses: genomic RNAs, transcription, and replication, p 139–149. *In* Oldstone MB (ed), *Arenaviruses I*. Springer-Verlag, Berlin, Germany.
 10. Burri DJ, da Palma JR, Kunz S, Pasquato A. 2012. Envelope glycoprotein of arenaviruses. *Viruses* 4:2162–2181.
 11. Borrow P, Oldstone MB. 1992. Characterization of lymphocytic choriomeningitis virus-binding protein(s): a candidate cellular receptor for the virus. *J. Virol.* 66:7270–7281.
 12. Eschli B, Quirin K, Wepf A, Weber J, Zinkernagel R, Hengartner H. 2006. Identification of an N-terminal trimeric coiled-coil core within arenavirus glycoprotein 2 permits assignment to class I viral fusion proteins. *J. Virol.* 80:5897–5907.
 13. Igonet S, Vaney MC, Vohnrein C, Bricogne G, Stura EA, Hengartner H, Eschli B, Rey FA. 2011. X-ray structure of the arenavirus glycoprotein GP2 in its postfusion hairpin conformation. *Proc. Natl. Acad. Sci. U. S. A.* 108:19967–19972.
 14. Cao W, Henry MD, Borrow P, Yamada H, Elder JH, Ravkov EV, Nichol ST, Compans RW, Campbell KP, Oldstone MB. 1998. Identification of alpha-dystroglycan as a receptor for lymphocytic choriomeningitis virus and Lassa fever virus. *Science* 282:2079–2081.
 15. Oldstone MB, Campbell KP. 2011. Decoding arenavirus pathogenesis: essential roles for alpha-dystroglycan-virus interactions and the immune response. *Virology* 411:170–179.
 16. Shimojima M, Stroher U, Ebihara H, Feldmann H, Kawaoka Y. 2012. Identification of cell surface molecules involved in dystroglycan-independent lassa virus cell entry. *J. Virol.* 86:2067–2078.
 17. van Kooyk Y. 2008. C-type lectins on dendritic cells: key modulators for the induction of immune responses. *Biochem. Soc. Trans.* 36:1478–1481.
 18. Svajcer U, Anderlueh M, Jeras M, Obermajer N. 2010. C-type lectin DC-SIGN: an adhesion, signalling and antigen-uptake molecule that guides dendritic cells in immunity. *Cell. Signalling* 22:1397–1405.
 19. McGreal EP, Miller JL, Gordon S. 2005. Ligand recognition by antigen-presenting cell C-type lectin receptors. *Curr. Opin. Immunol.* 17:18–24.
 20. Geijtenbeek TB, Kwon DS, Torensma R, van Vliet SJ, van Duinhoven GC, Middel J, Cornelissen IL, Nottet HS, KewalRamani VN, Littman DR, Figdor CG, van Kooyk Y. 2000. DC-SIGN, a dendritic cell-specific HIV-1-binding protein that enhances trans-infection of T cells. *Cell* 100:587–597.
 21. Kwon DS, Gregorio G, Bitton N, Hendrickson WA, Littman DR. 2002. DC-SIGN-mediated internalization of HIV is required for trans-enhancement of T cell infection. *Immunity* 16:135–144.
 22. Alvarez CP, Lasala F, Carrillo J, Muniz O, Corbi AL, Delgado R. 2002. C-type lectins DC-SIGN and L-SIGN mediate cellular entry by Ebola virus in cis and in trans. *J. Virol.* 76:6841–6844.
 23. Simmons G, Reeves JD, Grogan C, Vandenberghe LH, Baribaud F, Whitbeck JC, Burke E, Buchmeier MJ, Soilleux EJ, Riley JL, Doms RW, Bates P, Pohlmann S. 2003. DC-SIGN and DC-SIGNR bind ebola glycoproteins and enhance infection of macrophages and endothelial cells. *Virology* 305:115–123.
 24. Jeffers SA, Tusell SM, Gillim-Ross L, Hemmila EM, Achenbach JE, Babcock GJ, Thomas WD, Jr, Thackray LB, Young MD, Mason RJ, Ambrosino DM, Wentworth DE, Demartini JC, Holmes KV. 2004. CD209L (L-SIGN) is a receptor for severe acute respiratory syndrome coronavirus. *Proc. Natl. Acad. Sci. U. S. A.* 101:15748–15753.
 25. Tassaneeritthep B, Burgess TH, Granelli-Piperno A, Trumpfheller C, Finke J, Sun W, Eller MA, Pattanapanyasat K, Sarasombath S, Birx DL, Steinman RM, Schlesinger S, Marovich MA. 2003. DC-SIGN (CD209) mediates dengue virus infection of human dendritic cells. *J. Exp. Med.* 197:823–829.
 26. Navarro-Sanchez E, Altmeyer R, Amara A, Schwartz O, Fieschi F, Virelizier JL, Arenzana-Seisdedos F, Despres P. 2003. Dendritic-cell-specific ICAM3-grabbing non-integrin is essential for the productive infection of human dendritic cells by mosquito-cell-derived dengue viruses. *EMBO Rep.* 4:723–728.
 27. Davis CW, Nguyen HY, Hanna SL, Sanchez MD, Doms RW, Pierson TC. 2006. West Nile virus discriminates between DC-SIGN and DC-SIGNR for cellular attachment and infection. *J. Virol.* 80:1290–1301.
 28. Lozach PY, Kuhbacher A, Meier R, Mancini R, Bitto D, Bouloy M, Helenius A. 2011. DC-SIGN as a receptor for phleboviruses. *Cell Host Microbe* 10:75–88.
 29. Buchmeier MJ, Lewicki HA, Tomori O, Oldstone MB. 1981. Monoclonal antibodies to lymphocytic choriomeningitis and pichinde viruses: generation, characterization, and cross-reactivity with other arenaviruses. *Virology* 113:73–85.
 30. Weber EL, Buchmeier MJ. 1988. Fine mapping of a peptide sequence containing an antigenic site conserved among arenaviruses. *Virology* 164:30–38.
 31. Lozach PY, Mancini R, Bitto D, Meier R, Oestereich L, Overby AK, Pettersson RF, Helenius A. 2010. Entry of bunyaviruses into mammalian cells. *Cell Host Microbe* 7:488–499.
 32. Kunz S, Rojek JM, Kanagawa M, Spiropoulou CF, Barresi R, Campbell KP, Oldstone MB. 2005. Posttranslational modification of alpha-dystroglycan, the cellular receptor for arenaviruses, by the glycosyltransferase LARGE is critical for virus binding. *J. Virol.* 79:14282–14296.
 33. Scutera S, Fraone T, Musso T, Cappello P, Rossi S, Pierobon D, Orinska Z, Paus R, Bulfone-Paus S, Giovarelli M. 2009. Survival and migration of human dendritic cells are regulated by an IFN-alpha-inducible Axl/Gas6 pathway. *J. Immunol.* 183:3004–3013.
 34. Lozach PY, Burtleigh L, Staropoli I, Navarro-Sanchez E, Harriague J, Virelizier JL, Rey FA, Despres P, Arenzana-Seisdedos F, Amara A. 2005. Dendritic cell-specific intercellular adhesion molecule 3-grabbing non-integrin (DC-SIGN)-mediated enhancement of dengue virus infection is independent of DC-SIGN internalization signals. *J. Biol. Chem.* 280:23698–23708.
 35. Gramberg T, Soilleux E, Fisch T, Lalor PF, Hofmann H, Wheeldon S, Cotterill A, Wegele A, Winkler T, Adams DH, Pohlmann S. 2008. Interactions of LSECtin and DC-SIGN/DC-SIGNR with viral ligands: differential pH dependence, internalization and virion binding. *Virology* 373:189–201.
 36. Rojek JM, Sanchez AB, Nguyen NT, de la Torre JC, Kunz S. 2008. Different mechanisms of cell entry by human-pathogenic Old World and New World arenaviruses. *J. Virol.* 82:7677–7687.
 37. Pinschewer DD, Perez M, Sanchez AB, de la Torre JC. 2003. Recombinant lymphocytic choriomeningitis virus expressing vesicular stomatitis virus glycoprotein. *Proc. Natl. Acad. Sci. U. S. A.* 100:7895–7900.
 38. Perez M, Watanabe M, Whitt MA, de la Torre JC. 2001. N-terminal domain of Bornavirus protein G (p56) protein is sufficient for virus receptor recognition and cell entry. *J. Virol.* 75:7078–7085.
 39. Takada A, Robison C, Goto H, Sanchez A, Murti KG, Whitt MA, Kawaoka Y. 1997. A system for functional analysis of Ebola virus glycoprotein. *Proc. Natl. Acad. Sci. U. S. A.* 94:14764–14769.
 40. Dutko FJ, Oldstone MB. 1983. Genomic and biological variation among commonly used lymphocytic choriomeningitis virus strains. *J. Gen. Virol.* 64:1689–1698.
 41. Pettersson R, Kaariainen L. 1973. The ribonucleic acids of Uukuniemi virus, a noncubic tick-borne arbovirus. *Virology* 56:608–619.
 42. Elliott LH, McCormick JB, Johnson KM. 1982. Inactivation of Lassa, Marburg, and Ebola viruses by gamma irradiation. *J. Clin. Microbiol.* 16:704–708.
 43. Rojek JM, Campbell KP, Oldstone MB, Kunz S. 2007. Old World arenavirus infection interferes with the expression of functional alpha-dystroglycan in the host cell. *Mol. Biol. Cell* 18:4493–4507.
 44. Kunz S, Sevilla N, Rojek JM, Oldstone MB. 2004. Use of alternative receptors different than alpha-dystroglycan by selected isolates of lymphocytic choriomeningitis virus. *Virology* 325:432–445.
 45. Pasqual G, Rojek JM, Masin M, Chatton JY, Kunz S. 2011. Old world arenaviruses enter the host cell via the multivesicular body and depend on the endosomal sorting complex required for transport. *PLoS Pathog.* 7:e1002232. doi:10.1371/journal.ppat.1002232.
 46. Rojek JM, Moraz ML, Pythoud C, Rothenberger S, Van der Goot FG, Campbell KP, Kunz S. 2012. Binding of Lassa virus perturbs extracellular matrix-induced signal transduction via dystroglycan. *Cell Microbiol.* 14:1122–1134.
 47. Lee AM, Cruite J, Welch MJ, Sullivan B, Oldstone MB. 2013. Pathogenesis of Lassa fever virus infection: I. Susceptibility of mice to recombinant Lassa Gp/LCMV chimeric virus. *Virology* 442:114–121.
 48. Walker DH, McCormick JB, Johnson KM, Webb PA, Komba-Kono G, Elliott LH, Gardner JJ. 1982. Pathologic and virologic study of fatal Lassa fever in man. *Am. J. Pathol.* 107:349–356.
 49. Burns JW, Buchmeier MJ. 1991. Protein-protein interactions in lymphocytic choriomeningitis virus. *Virology* 183:620–629.

50. Dominguez-Soto A, Aragonese-Fenoll L, Martin-Gayo E, Martinez-Prats L, Colmenares M, Naranjo-Gomez M, Borrás FE, Muñoz P, Zubiaur M, Toribio ML, Delgado R, Corbi AL. 2007. The DC-SIGN-related lectin LSECtin mediates antigen capture and pathogen binding by human myeloid cells. *Blood* **109**:5337–5345.
51. Ohkuma S, Poole B. 1978. Fluorescence probe measurement of the intralysosomal pH in living cells and the perturbation of pH by various agents. *Proc. Natl. Acad. Sci. U. S. A.* **75**:3327–3331.
52. Ohkuma S, Poole B. 1981. Cytoplasmic vacuolation of mouse peritoneal macrophages and the uptake into lysosomes of weakly basic substances. *J. Cell Biol.* **90**:656–664.
53. Johannsdottir HK, Mancini R, Kartenbeck J, Amato L, Helenius A. 2009. Host cell factors and functions involved in vesicular stomatitis virus entry. *J. Virol.* **83**:440–453.
54. Mercer J, Helenius A. 2009. Virus entry by macropinocytosis. *Nat. Cell Biol.* **11**:510–520.
55. Mercer J, Helenius A. 2008. Vaccinia virus uses macropinocytosis and apoptotic mimicry to enter host cells. *Science* **320**:531–535.
56. Raiborg C, Stenmark H. 2009. The ESCRT machinery in endosomal sorting of ubiquitylated membrane proteins. *Nature* **458**:445–452.
57. Illick MM, Branco LM, Fair JN, Illick KA, Matschiner A, Schoepp R, Garry RF, Guttieri MC. 2008. Uncoupling GP1 and GP2 expression in the Lassa virus glycoprotein complex: implications for GP1 ectodomain shedding. *Virol. J.* **5**:161.
58. Klewitz C, Klenk HD, ter Meulen J. 2007. Amino acids from both N-terminal hydrophobic regions of the Lassa virus envelope glycoprotein GP-2 are critical for pH-dependent membrane fusion and infectivity. *J. Gen. Virol.* **88**:2320–2328.
59. Cosset FL, Marianneau P, Verney G, Gallais F, Tordo N, Pecheur EL, ter Meulen J, Deubel V, Bartosch B. 2009. Characterization of Lassa virus cell entry and neutralization with Lassa virus pseudoparticles. *J. Virol.* **83**:3228–3237.
60. Kanagawa M, Saito F, Kunz S, Yoshida-Moriguchi T, Barresi R, Kobayashi YM, Muschler J, Dumanski JP, Michele DE, Oldstone MB, Campbell KP. 2004. Molecular recognition by LARGE is essential for expression of functional dystroglycan. *Cell* **117**:953–964.
61. Barresi R, Campbell KP. 2006. Dystroglycan: from biosynthesis to pathogenesis of human disease. *J. Cell Sci.* **119**:199–207.
62. Rojek JM, Spiropoulou CF, Campbell KP, Kunz S. 2007. Old World and clade C New World arenaviruses mimic the molecular mechanism of receptor recognition used by alpha-dystroglycan's host-derived ligands. *J. Virol.* **81**:5685–5695.